Published in final edited form as:

Cancer Res. 2017 November 01; 77(21): 5977–5988. doi:10.1158/0008-5472.CAN-17-0064.

Tenascin-C and integrin α9 mediate interactions of prostate cancer with the bone microenvironment

Rebeca San Martin[1], **Ravi Pathak**[5], **Antrix Jain**[1], **Sung Yun Jung**[2], **Susan G. Hilsenbeck**[3], **María C. Piña-Barba**[4], **Andrew G. Sikora**[5], **Kenneth J. Pienta**[6], **David R. Rowley**[1]

[1]The Department of Molecular and Cellular Biology. Baylor College of Medicine

[2]Department of Biochemistry and Molecular Biology. Baylor College of Medicine

[3]Biostatistics and Informatics Shared Resource Duncan Cancer Center

[4]Laboratorio de Biomateriales. Instituto de Investigaciones en Materiales. Universidad Nacional Autónoma de México. Av. Universidad 3000, Copilco, Ciudad de México, 04510 Mexico

[5]Bobby R. Alford Department of Otolaryngology - Head and Neck Surgery, Baylor College of Medicine. One Baylor Plaza, Houston, TX, 77030. USA

[6]The James Buchanan Brady Urological Institute, Johns Hopkins University School of Medicine. 600 North Wolfe Street, Baltimore, Maryland 21287. USA

Abstract

Deposition of the extracellular matrix protein tenascin-C is part of the reactive stroma response, which has a critical role in prostate cancer progression. Here we report that tenascin-C is expressed in the bone endosteum and involved associated with formation of prostate bone metastases. Metastatic cells cultured on osteo-mimetic surfaces coated with tenascin-C exhibited enhanced adhesion and colony formation as mediated by integrin α9β1. Additionally, metastatic cells preferentially migrated and colonized tenascin-C-coated trabecular bone xenografts in a novel system that employed chorioallantoic membranes of fertilized chicken eggs as host. Overall, our studies deepen knowledge about reactive stroma responses in the bone endosteum that accompany prostate cancer metastasis to trabecular bone, with potential implications to therapeutically target this process in patients.

Keywords

Bone metastasis; tenascin-C; integrin alpha 9

INTRODUCTION

Local prostate cancer (PCa) that progresses and invades outside the gland preferentially metastasizes to bone among other tissues (1). The formation of new micro metastases and the subsequent growth of macroscopic tumors results in bone pain and potentially pathologic

Correspondence: David R. Rowley, Baylor College of Medicine, One Baylor Plaza 514B, Houston, Texas 77030. United States, drowley@bcm.edu.

fracture. These metastases are primarily osteoblastic. The specific mechanisms that promote metastasis to bone are not understood, however, the role of the microenvironment in bone has been proposed as an important player in this process (1). Specifically, the mechanisms that mediate colonization of prostate cancer cells to the bone endosteum and then promote colony expansion are essentially unknown, however alterations in adhesion have been shown to affect metastatic potential (2). The bone endosteum is a layer of cells lining the internal trabecular bone and is composed of osteoprogenitor stem cells, resting and active osteoblasts, and osteoclasts. The endosteum is the site of the osteoblastic niche in bone, which has been shown to be important for hematopoietic stem cells self-renewal (3). Importantly, this same endosteal osteoblastic niche has been shown to be the site of prostate cancer metastases and data suggests that prostate cancer cells compete with hematopoietic stem cells for this niche (4).

Tenascin-C is a hexameric extracellular matrix protein that is evolutionary conserved in the order *Chordata* (5) and plays an essential role in the development of bone and the nervous system (6,7). Interestingly, the expression of tenascin-C in adult, differentiated tissues at homeostasis is negligible, but its deposition is essential for wound repair (8–10). Importantly, tenascin-C is expressed at sites of new bone deposition by osteoblasts (11). During bone development, tenascin-C was found in osteogenic cells that invade cartilage during endochondral ossification and in the condensed osteogenic mesenchyme that form new bone during intramembranous ossification and around new bone spicules. These studies also showed that after bone formation, some tenascin-C remains located in the endosteum surface; however, it is not found in the mature bone matrix (12). Important to the results of the present study, elevated tenascin-C deposition is observed at sites of bone repair after fractures (13).

In prostate cancer, tenascin-C is deposited early during cancer progression and is a key hallmark of reactive stroma (14). Reactive stroma recapitulates a normal wound repair (15), and is composed of a heterogeneous population of vimentin positive cancer associated fibroblasts (CAFs) and myofibroblasts; cells derived from tissue-resident MSC that express smooth muscle alpha actin and vimentin (VIM) upon the influence of TGF-beta (16). This tenascin-C enrichment of the tumor microenvironment affects cancer cell adhesion, migration and proliferation (17). In this context, tenascin-c also exhibits immune suppressive functions in tumors via regulation of cytokine/chemokine expression that affects inflammation and the immune landscape (18).

The reactive stroma response in prostate cancer initiates early in the disease, during prostatic intraepithelial neoplasia (PIN)(19) and is predictive of biochemical recurrence after prostatectomy (20). Persistent deposition of tenascin-C by both CAFs and myofibroblasts (21) may foster the progression of prostate cancer and initiation of metastasis via differential adhesion patterns and transient EMT induction (22).

In the case of prostate cancer, metastases preferentially target bone (23). Following Paget's "seed and soil" hypothesis (24), the colonization of a secondary site by a cancer cell that has successfully escaped the primary tumor site is dependent on a suitable environment amenable to colonization. Therefore, the possibility arises that metastatic colonization

initiates a reactive response at the secondary site (25), and/or an underlying pathology at the secondary site created a “fertile soil” in which the metastatic foci preferentially colonizes. Interestingly, the microenvironment changes present in prostate cancer bone metastases, in the context of a reactive tissue phenotype, have not been characterized.

We report here a spatial association of human prostate cancer bone metastases with reactive endosteum foci high in tenascin-C deposition and dissect the role of tenascin-C in regulating adhesion and colony initiation. Selective adhesion and colony formation on bone/tenascin-C surfaces was mediated by integrin α9β1 in prostate cancer cells in novel human 3D osteogenic organoids and in egg chorioallantoic membrane metastasis models that use tenascin-C coated, humanized, bovine trabecular bone cubes. This work extends our understanding of bone metastasis mechanisms in prostate cancer and identifies α9 integrin - tenascin-C interaction as a key mediator.

MATERIALS AND METHODS

Bone Metastasis Tissue Microarray

Human bone metastasis tissue microarrays were constructed from the rapid autopsy program at University of Michigan. TMA#85 contains 63 bone metastases samples, six liver metastasis samples, three lung metastasis samples, and twelve prostate cancer samples, representing a total of 32 patients. Tissue samples from bone metastasis include 10 patients with bone marrow-associated lesions and 12 patients with Trabeculae associated metastatic foci (in triplicate). This array was analyzed via immunohistochemistry for the reactive stroma markers tenascin-C, pro-collagen I, smooth muscle alpha actin, vimentin, and immune cell makers CD14 and CD68 (supplemental experimental procedures, supplemental tables 1-2)

In Vitro MSC-Derived 3D Endosteal Organoid Model

Human adult mesenchymal stem cells (MSCs, Lonza) growing in T75 cell culture flasks were trypsinized using standard protocols and washed twice with 10 ml of BFS media (supplemental experimental procedures) by centrifugation (400 rpm, 3 min). The cell pellet was re-suspended in BFS media to a concentration of 400,000 cells/300 μl or 800,000 cells/300 μl. Cell culture inserts (Millipore. Millicell-CM 12mm) were prepared as suggested by the manufacturer and each chamber was seeded with 300 μl of the cell suspension. After overnight incubation, once MSC spheroids were formed, the BFS media in both the inner and outer chambers was substituted with complete osteogenic media (R&D CCM007 supplemented with CCM008). Osteogenic organoids were cultured for 7, 14, and 21 days, with media changes every two days. Control organoids were kept in BFS media for the appropriate time points, with media changes every two days.

For cancer co-culture experiments, the media inside the insert was substituted with 300 μl of cancer cell-specific media containing 4×10^5cells (LNCaP, VCaP or PC3), and the media outside each insert was replaced with 600 μl of the same media, as needed. Control organoids were exposed to cancer-cell media alone. After 24 hours of incubation at 37°C, 5% CO_2, the media in the outside chamber was replaced with fresh media. Co culture

samples were harvested after 48 hours and processed for histology and immunohistochemistry (supplemental experimental procedures, supplemental table 3)

In vitro Trabecular Bone Scaffold culture system.

Nukbone ® (Biocriss S.A. de C.V. Mexico) bovine trabecular bone scaffolds, in either 200–500 μm particles or 0.5 cm cube were coated with human, full length tenascin-C (Millipore Cat. No. CC06) or BSA control, by immersion of the bone fragments into a 100 μg/ml solution of either protein for seven days. Coating was confirmed by immunohistochemistry (Supplemental experimental procedures). For in vitro adhesion and proliferation experiments, coated NukBone ® cubes were cultured with 250,000 VCaP cells in DMEM/F-12 1:1 (Invitrogen) containing 0.1% BSA, without antibiotics, using non-adhesive (CM) inserts as described before.

Prostate Cancer Cell Lines Adhesion to Tenascin-C

Tenascin-C coating was done according to published protocols (26), with modifications. Using a 0.5 mm cutting template (ICN Cat No 4215), we scored circles on the outside of the bottom of the cell culture wells (Osteo Assay surface, 24 well plates. Cat. No. 3987 Corning® or Costar ® Non-treated, 6 well plates). In the case of the 6 well plate, 3 circles per well were inscribed. These circles were used as guides for microscopical analysis of coated surfaces. For coating, a 3 μl drop of human, full length purified Tenascin-C (Millipore Cat. No. CC06) at the appropriate concentration (0, 5, 10, 25, 50, 75, and 100 μg/ml), in PBS pH 7.4, was applied in the center of each of the circles, and incubated 48 hours at 37°C, until the droplets dried out. BSA at the appropriate concentrations was coated as control. Tenascin-C coating was verified as follows: coated wells were incubated for 72 hours in DMEM/F-12 1:1 (Invitrogen) containing 0.1% BSA, without antibiotics at 37°C and 5% CO_2. Plates were then fixed with 4% paraformaldehyde for 20 min at room temperature and tenascin-C was detected via immunocytochemistry (AP-Vector Blue, supplemental experimental procedures).

Cells (VCaP, PC3 and LNCaP) were seeded at a density of 1×10^5 cells/cm^2 in their basal media (DMEM/F-12 1:1 or RPMI) containing 0.1% BSA, without antibiotics. Cells were allowed to adhere for 3 hours at 37°C and 5% CO_2 before washing all wells three times with warm media. For imaging of adherent cells, fifteen micrographs at a 10X magnification were acquired for each of the experimental conditions, making sure to image more than 90% of the coated areas, quantification was performed with the cell counter function in the Image J software (27).

Neutralizing of integrin α9β1 activity.—Integrin neutralization was done as according to published protocols (28). In brief, VCaP cells were incubated in DMEM/F-12 1:1 (Invitrogen) containing 0.1% BSA, supplemented with α9β1 neutralizing antibody, clone Y9A2 (Biolegend cat. No. 351603) or mouse isotype control (Mouse IgG, Sigma-Aldrich cat. No. I5381), at a concentration of 10 μg/ml for 30 min on ice before being seeded onto the tenascin-C coated surfaces at a density of 2.2×10^5 cells/cm^2. As described before, cells were allowed to adhere for 3 hr. before washing the wells and quantification of adherent

cells. Knockdown of α9 expression via siRNA was conducted and verified as outlined in the Supplemental experimental procedures (Supplemental table 4).

CAM – Humanized Bovine Bone Integrated Experimental System

This system used the chorioallantoic membrane (CAM) of the chicken egg as a host for a xenograft composed of the "humanized" NukBone ® in combination with an organoid consisting of a mixture of VCaP cells (prostate cancer metastatic cell line) and the prostate-derived mesenchymal stem cell hpMSC19I (16). Briefly, 8-day-old pathogen-free embryonated eggs were prepared as previously described (29) to expose the CAM. A neoprene ring was installed on top of the exposed CAM to delimit the xenograft location, and 100 μl of attachment factor (Gibco) was added in the chamber and allowed to set. The trabecular bone cube, coated with human tenascin-CC, is placed on top. The prostate cell line-derived organoid (Supplemental Experimental Procedures) is deposited on this surface as well, about 0.5 cm away from the bone scaffold. The egg is then placed in a humidity-controlled incubator at 37°C for six days. Xenograft-bearing eggs were then incubated on ice for 20 min to anesthetize the chick. Using a syringe equipped with an 18-gauge needle, 3 ml of ice cold 4% paraformaldehyde was carefully injected through the taped window, to prevent contamination and touching the CAM/sample, to overlay the fixative over the CAM. Eggs were incubated on ice for a total of 4 hours to euthanize the chicks. The CAM was then dissected out in bulk. Tissues were placed in a 4-cm glass-bottomed cell culture dish (MatTek P35G-0–20-C) containing 5 ml of cold 4% paraformaldehyde and incubated at 4°C over night without shaking. Tissues were then washed with three changes of PBS (5 ml each) for 5 minutes. Samples were then decalcified, paraffin embedded and sectioned (Supplemental Experimental Procedures) taking care of embedding the xenograft with the CAM in the most proximal side of the block. For analysis of metastatic colonization of the trabecular bone fragment, 120 serial sections were acquired from each block, at a nominal thickness of 5 μm, collecting two sections per slide for a total of 60 slides. One out of every eight slides were then stained with hematoxylin and eosin (H&E). Following microscopic evaluation for epithelial pockets associated with the bone, adjacent sections were analyzed by immunohistochemistry studies to verify epithelial origin (pan-cytokeratin), and markers of interest (human ITGA9). Number of foci per sample were counted based on the following rubric: metastatic epithelial foci is defined as a) a collection of cuboidal cells that form clusters on the surface of the trabecular bone or b) a layer of cuboidal cells, in direct contact with the trabecular surface. Layers and clusters of cells, as previously described, that associated to different trabeculae and were at least 200 microns apart were counted as two separate foci. Layers and clusters of cells that associate to blood-like cells that rest atop the bone fragment were not considered as foci.

In-ovo experiments followed approved protocols from the Institutional Animal Care and Use Committee.

Statistical Analysis

Statistical analysis was carried out on Prism Software (Graph Pad).

Cell counts for adhesion experiments were analyzed using one way ANOVA with Tukey's multiple comparisons test. ***p<0.001, *p < 0.05

qRT-PCR analysis was analyzed by two-way ANOVA. n = 3; *P < 0.05; **P < 0.01; ***P < 0.001.

CAM-Trabecular bone xenografts foci count data was analyzed using Student's t test with Welch correction ***p<0.001.

RESULTS

Identification of a Reactive Endosteum Phenotype in Trabeculae-Associated Metastatic Foci of Human Prostate Cancer.

To assess a reactive phenotype in the context of bone metastasis, a human prostate cancer bone metastasis tissue array (TMA85 array, 63 metastasis samples, University of Michigan) was evaluated using dual immunohistochemistry protocols as follows: Tenascin-C/vimentin, smooth muscle alpha-actin/vimentin, pro collagen I/vimentin, as well as immunohistochemistry for the immune markers CD14 and CD68 (Supplemental experimental procedures). Image analysis revealed the bone metastasis can be classified into two distinct groups: a) metastatic foci associated directly with the trabecular bone surface and b) metastatic foci associated with a reactive marrow stroma but not on the bone surface. Foci on the bone surface were associated with elevated immunoreactivity for tenascin-C in the endosteum (Figure 1A, B), whereas smooth muscle alpha-actin staining was negligible (Figure 1C). Of the 15 patients with trabeculae-associated metastasis, 11 showed trabecular TNC deposition in at least two of the three samples present in the array (73%). Adjacent areas immunoreactive to pro collagen I were observed in 69% of tenascin-C positive foci (Figure 1B), with varying degrees of staining intensity from absent (Supplemental Figure 1A) to high (Supplemental figure 1B-D). We subsequently termed this the reactive endosteum phenotype. In contrast, bone marrow associated metastatic foci were negative for tenascin-C and procollagen deposition, and showed a substantial immunoreactivity to smooth muscle alpha-actin in associated blood vessels (Figure 1C). Elevated staining intensities of CD14 (Supplemental Figure 2A). and CD68 macrophages (Supplemental Figure 2B) were also observed in trabeculae associated metastasis, when compared with marrow associated foci.

Differentiation of Mesenchymal Stem Cells in non-Adhesive Conditions Produces 3D Osteogenic Organoids.

To evaluate interactions of an activated endosteum and prostate cancer metastatic cell lines, a human 3D osteogenic organoid model was generated. At seven days of osteogenic induction in non-adherent conditions, human mesenchymal stem cells generated spheroids that differentiated into hard, white, opalescent organoids. These organoids were apparently tethered to the sides of the cell culture insert by distinct, fibrous, and flexible tendrils (Figure 2A). Histological analysis of 3D organoids revealed that a central mass of cells was surrounded by a flat and compact layer of outer cells that were nearly identical to the endosteum layer associated with trabecular bone (Figure 2A-H&E). These cells were

positive for osteocalcin, alkaline phosphatase, and osteonectin (SPARC), confirming osteoblast differentiation (Figure 2A). Interestingly, this layer was also positive for tenascin-C deposition (Figure 2A). Immunoreactivity to smooth alpha actin, while present in control organoids, was negative in osteo induced conditions (Supplemental Figure 3A, B). Finally, control 3D organoids retain a soft, loosely aggregated structure (Supplemental Figure 4A) with reduced viability as shown by TUNEL staining (Supplemental Figure 4B) and immunohistochemistry for cleaved caspase 3 (Supplemental Figure 4C).

Prostate Cancer Cell Lines Preferentially Adhere to Tenascin-C high foci in 3D Osteogenic Organoids.

Under co-culture conditions with the 3D osteogenic organoids, the prostate bone metastatic cell line VCaP, exhibited selective attachment to foci high in tenascin-C high, localized primarily on the endosteum tendrils (Figure 2B). Distinct branching of the endosteal tendrils around the cancer clusters was observed in some samples. In stark contrast, co-culture of the 3D organoids with the metastatic line PC-3, which is osteolytic, resulted degradation of the osteogenic organoid (Supplemental Figure 5A) creating holes in the matrix, and detachment of the endosteum tendrils from the culture vessel wall. Endosteum tendrils that remained showed the characteristic tenascin-C enrichment with clusters of cancer cells. LNCaP prostate cancer cells (derived from a lymph node metastasis) adhered to the surface of 3D osteogenic organoids and elicited a reactive degradation response of the endosteum manifested as furrows in the underlying matrix (Supplemental Figure 5B).

Prostate Cancer Metastatic Cells Adhere to Tenascin-C in a Dose-Dependent Manner.

To assess whether bone metastatic prostate cancer cell lines would adhere preferentially to tenascin-C, we used both non-treated, ultra-low adhesion cell culture plates and Osteo Assay plates (pre-treated with osteo-mimetic calcium phosphate) that were coated with increasing concentrations of human tenascin-C. A stable coating with tenascin-C was verified via immunocytochemistry (Figure 3A, B). At 3 hours of incubation in serum-free medium, we observed a differential and concentration-dependent adhesion of VCaP cells with an optimal adhesion observed with a coating of 75 μg/ml of tenascin-C (Figure 3C). Furthermore, adhering VCaP cells proliferated and formed three dimensional foci at 72 hours of culture in serum-free media conditions (Figure 3A, Supplemental Figure 6A). Interestingly, the osteoclastic cell line PC3, and the lymph node-derived cell line LNCaP did not show enhanced adhesion to tenascin-C under these conditions (Supplemental Figure 6B, C respectively), and adhere to the substrate at significantly lower levels than VCaP (Supplemental Figure 6D).

VCaP cells grown on tenascin-C coated Osteo Assay plates adhere readily to the surface, showing spreading as early as 3 hours after seeding (Figure 3B), and were also able to develop three dimensional foci at 72 hours of culture in serum free conditions. Cells seeded on tenascin-C coated osteo mimetic plates adhere and initiate proliferation upon seeding, whereas control cultures exhibit a lag time of approximately 15–18 hours (Figure 3D). Thereafter, both experimental and control cells proliferate at approximately the same rate. Cultures on tenascin-C plates also reach a higher population density compared to control, with both groups seeded in serum-free media (Figure 3D). In addition, elevated population

density was confirmed with VCaP cells seeded onto human tenascin-C coated trabecular bone scaffolds (NukBone ®) as compared to control conditions in both serum free and low-serum culture conditions (Supplemental Figures 7A, B respectively) as shown via MTT assay (Supplemental Figure 7C). These trabecular bone scaffolds (Supplemental Figure 8A) readily absorb a stable coating of tenascin-C (Supplemental Figure 8B). Finally, VCaP cells form three dimensional colonies on these tenascin-C-coated scaffolds in non-serum culture conditions (Supplemental Figure 8C)

Integrin α9β1 is Essential for Adhesion of Prostate Cancer-Derived Metastatic Cells to Tenascin-C

Owning to the rapid adhesion observed in both the low adhesion and osteo mimetic, tenascin-C coated cell culture conditions, we hypothesized that metastatic cell lines exhibited integrin profiles that mediated interaction with tenascin-C. Thus, a cohort of prostate cell lines (PNT1A, BPH1, LNCaP, VCaP, PC3, 22RV1, Du145, and LNCaP C4–2B) were profiled for expression of integrins known to mediate tenascin-C binding. A relatively high expression level of α9 integrin was noted in VCaP cells (Figure 4A and Supplemental Figures 9-10), which was later confirmed via immunohistochemistry for the α9β1 dimer in cells associated with 3D osteogenic organoids (Figure 4B). Further, IHC analysis showed cells immunoreactive to integrin α9 in 74% of the cancer foci associated with tenascin-C in the TMA85 tissue array samples (Figure 4C). Finally, both neutralization of the α9β1 integrin dimer via neutralizing antibodies (Figure 4D, E) and knockdown of the α9 subunit gene expression with siRNA (Figure 4F-G, Supplemental Figure 11A-B, Supplemental Table 5, and experimental procedures), ablated VCaP adhesion to tenascin-C coated osteo mimetic surfaces. Together, these data support the hypothesis that the α9β1 integrin plays an important role in the adhesion and colonization of prostate cancer cells in the bone metastatic niche.

Tenascin-C Induces Chemotaxis and Colony Formation of VCaP in a Chorioallantoic Membrane (CAM) – Humanized Bovine Bone Integrated Experimental System

To model the interactions between reactive endosteum on trabecular bone and metastatic cancer cells, we developed an *in ovo* xenograft system in which a human tenascin-C-coated trabecular bovine cube was co-cultured in close proximity to an organoid (Figure 5A) comprised of bone metastatic cells (VCaP) and human prostate-derived mesenchymal stem cells (hpMSC 19-I) on a chicken egg chorioallantoic membrane (CAM).

A mixture of VCAP and of hpMSC19I was cultured overnight under non-adhesive conditions to produce 3D organoids as we have reported previously (16) (Supplemental Experimental Procedures). This mixture of cells starts contraction and segregation into distinct epithelial and stromal compartments as early as three hours after seeding (Figure 5A, B, C). At this early time point, it is possible to detect the epithelial compartment via immunohistochemistry for pan cytokeratin and androgen receptor (AR) (Figure 5D). These 3D organoids were placed on the CAM of the fertilized chicken egg, along with Nukbone ® bovine trabecular bone cubes coated with either tenascin-C or BSA as control, as previously described (Figure 5E, F).

After six days of *in ovo* incubation, trabecular bone cubes recruited CAM blood vessels that infiltrate into the trabecular bone cube in a tenascin-C independent manner (Figure 5G). Tenascin-C coated trabecular bone cubes show colonization of VCaP cells, identified by expression of human α9 integrin, indicating these cells migrated from the organoid towards to scaffold (Figure 5 H, I). Quantification of foci revealed that VCaP preferentially migrate to tenascin-C coated bone fragments as compared with BSA coated controls (Figure 5J).

Tenascin-C Elicits the Production of Collagen XIIa1 in Metastatic Prostate Cells.

To assess potential downstream effectors of tenascin-C induced biology, two-dimensional RP/LC-MS analysis in VCaP cells cultured on tenascin-C coated Osteo Assay plates was conducted (Supplemental Experimental Procedures). An increase in production of Laminin Subunit Beta 2 (LAMB2), Optineurin (OPTN), Golgi Associated, Gamma Adaptin Ear Containing, ARF Binding Protein 1 (GGA1), Phospholipase D Family Member 3 (PLD3) and Palmitoyl-Protein Thioesterase 2 (PPT2) was observed (Figure 6A). Of relevance, a distinct increase (30-fold) of collagen12, alpha1 (COL12A1) protein was noted and subsequently confirmed in VCaP grown on 3D osteogenic organoids using IHC (Figure 6B). Ablation of adhesion to tenascin-Coated osteo plates via siRNA knock down of integrin α9 resulted in a decrease of transcript for COL12A1 in VCaP cells cultured on tenascin-C coated osteo mimetic surfaces (Figure 6C), suggesting a direct link between cell binding and this osteogenic collagen production by the epithelial cell.

DISCUSSION.

We report a reactive endosteum phenotype that accompanies trabecular bone-associated prostate cancer metastasis, characterized by elevated deposition of tenascin-C and collagen I. Although its expression is limited in adult differentiated bone, tenascin-C plays an essential role in bone repair processes such as the formation of granulation tissue during fracture repair, in osteogenic differentiation, mineralization and bone remodeling due to mechanical load (13,30,31). Further, bone stromal cells and osteoblasts show increased tenascin-c expression upon in vitro co-culture with prostate cancer-derived cell lines (32) suggesting that tenascin-c deposition could arise as a response to metastatic colonization. It has been previously suggested that prostate metastatic cells compete with hematopoietic stem cells for their niche in bone (33), a niche that has been shown to be enriched in tenascin-C during activation (34). Our studies show that bone metastatic prostate cancer cells differentially adhere, proliferate more rapidly and form 3D colonies in tenascin-C coated osteo mimetic surfaces. Further, in a 3D osteogenic organoid model, prostate cancer cells preferentially attach at sites high in tenascin-C *in vitro* and tenascin-C coated bone fragments show enhanced metastatic colonization in an *in ovo* xenograft approach.

It is also important to note that the interaction of integrins with tenascin-C is mediated through the IDG and RGD sequences within the third fibronectin type III repeat in human tenascin-C (35). Of interest, the fibronectin type III repeat of mouse tenascin-C lacks the IDG and RGD sequences (35). It is possible that lack of these sequences in mouse tenascin-C may explain, in part, why transgenic mouse models of cancer rarely metastasize to bone or why injection of human cancer cells in immune compromised mice rarely metastasize to

bone. In contrast, studies where human fetal bone fragments were implanted into SCID mice showed preferential metastasis of tail vein-injected human prostate cancer cells to human bone fragments as compared with implanted mouse bone or endogenous mouse skeleton (36). In light of our results, this is not surprising, as tenascin-C expression is high in fetal human bone (11,12).

Repetitive bone loading in normal life leads to microscopic cracks or micro fractures in bone that undergoes subsequent bone repair processes. In humans, these micro fractures increase with age in an exponential manner (37). Tenascin-C is overexpressed in endosteum undergoing bone repair (13). In many cancer foci, we observed elevated tenascin-C deposition in the endosteum of the trabeculae represented in the section, not just in the immediate region occupied by foci of cancer cells. It is possible that prostate cancer cells preferentially colonize the tenascin-C high reactive endosteum of bone trabeculae that are undergoing the normal process of micro fracture repair as a function of aging. In this scenario, data reported here might suggest that cancer cells may not induce the reactive endosteum, rather an existing micro fracture-associated reactive endosteum is a preferential site for seeding of metastatic cells and colony initiation / formation. Since tenascin-C is highly deposited in the reactive stroma of primary prostate cancers (14), it's possible that cancer cells acquire a tenascin-C addiction prior to metastasis to bone.

It is estimated that 15% of the male population will develop invasive prostate cancer in the United States (38). In most cases, resection of the primary tumor and concomitant therapies grants a fifteen-year recurrence-free survival. Biochemical recurrence, as refers to elevated prostate specific antigen (PSA) levels is usually the first sign of prostate cancer progression, which is followed by distant metastasis in about 5% of patients. Interestingly, distant metastasis occurs 8–10 years after biochemical recurrence (39). The mechanisms that mediate this delay in metastatic development are not understood. Evidence suggests that tumor cells disseminate from prostate cancer in as many as 25% of patients with localized disease and that higher concentrations of these cells in blood negatively correlate with survival (40). However, it has been proposed that disseminated cancer cells become dormant in the secondary site microenvironment through several mechanisms (41,42). We propose that the tenascin-C rich osteo environments used throughout our study model a normal age-related or androgen ablation-induced bone loss (43,44) and/or subsequent incidence of subclinical micro-fractures. In this context, production of tenascin-C necessary for repair occurring at proximal site to a dormant foci might trigger their escape from dormancy, via differential cellular adhesion, consistent with previous findings (45).

Importantly, this study also provides evidence that metastatic prostate cancer cells interact with tenascin-C in the endosteum via the integrin α9β1 dimer (ITGA9 – ITGB1), as ablation of its activity via siRNA or neutralizing antibodies inhibits cell spreading on tenascin-C coated osteo surfaces. Further, integrin α9 positive cells are present at prostate metastatic foci enriched with tenascin-C in human samples (Figure 5). Integrin α9β1 has been previously implicated in the induction of metastatic phenotypes in cancers where the primary tumor is also enriched in tenascin-C expression, such as breast (46–48), lung (49) and colon (50). Of key interest, α9β1 mediates the interaction between the hematopoietic stem cell and a tenascin-C -rich niche in the endosteum (34). Integrin α9β1 also plays a

critical role in extravasation of neutrophils (51). Hence, the same integrin identified in the present study has been shown to mediate extravasation events and bone marrow colonization events in other normal cell types.

We also show here a significant induction in COL12A1 production by a prostate epithelial metastatic cell line (VCaP), which results from contact with tenascin-C on osteo mimetic surfaces. Collagen XIIa (COL12A1) is a member of the fibri-associated collagens with interrupted triple helices (FACIT) family, where it contributes to the organization and mechanical properties of collagen fibrils (52). COL12A1 is present throughout mesenchymal tissues during development, but it is restricted to fascia and basement membranes in dermis, kidney and muscle in adult organisms; a distribution that is conserved throughout vertebrate species (53). In bone development, a knock out mouse model for COL12A1 shows shorter, thinner long bones with low mechanical strength as well as decreased bone matrix deposition (54). COL12A null osteoblasts differentiate slower with poor mineralization, showing abnormal polarization; a role in the establishment of cell-cell interactions during bone formation has been implicated (55). Given the predominantly osteoblastic nature of prostate cancer is enticing to hypothesize that tenascin-C induced production of COL12A1 in metastatic cells would stimulate osteoblast differentiation and osteoid deposition at metastatic sites.

In conclusion, given that the reactive microenvironment response is essential for prostate cancer progression our work on characterizing the reactive response in the bone microenvironment, and what effect it has on metastasis addresses a major gap in the field. Hereof, we identify tenascin-C as an extracellular component of the osteoblastic niche that fosters the colonization and growth of trabecular-associated bone metastasis. In vitro and in vivo studies established that metastatic cells bearing integrin $\alpha 9\beta 1$ selectively migrate and colonize bone enriched in tenascin-C, suggesting that therapies aimed at blocking this axis will positively impact the outcome for patients with metastatic prostate cancer.

Supplementary Material

Refer to Web version on PubMed Central for supplementary material.

ACKNOWLEDGEMENTS

We thank Truong Dang and William Bingman III for technical assistance.

Financial Support:

This work is funded by grants from CRPIT RP140616 (D.R. Rowley), NIH NCI U01CA143055 (D.R. Rowley and K.J. Pienta), R01CA58093 (D.R. Rowley.), the Caroline Weiss Law Endowment (to A.G. Sikora), the CPRIT Proteomics and Metabolomics Core Facility Award RP12009, CCSG P30CA125123, and the Comprehensive Cancer Center Grant NIH NCI P30CA125123 to Baylor College of Medicine.

Abbreviations List:

CAF	Cancer associated fibroblast
CAM	Chorioallantoic membrane

COL12A1	Collagen XIIa1
MSC	Mesenchymal stem cell
PCa	Prostate Cancer
PIN	Prostatic intraepithelial neoplasia
TNC	Tenascin-C

REFERENCES

1. Jin JK, Dayyani F, Gallick GE. Steps in prostate cancer progression that lead to bone metastasis. Int J Cancer 2011;128(11):2545–61 doi 10.1002/ijc.26024. [PubMed: 21365645]
2. Lee YC, Bilen MA, Yu G, Lin SC, Huang CF, Ortiz A, et al. Inhibition of cell adhesion by a cadherin-11 antibody thwarts bone metastasis. Mol Cancer Res 2013;11(11):1401–11 doi 10.1158/1541-7786.MCR-13-0108. [PubMed: 23913163]
3. Calvi LM, Adams GB, Weibrecht KW, Weber JM, Olson DP, Knight MC, et al. Osteoblastic cells regulate the haematopoietic stem cell niche. Nature 2003;425(6960):841–6 doi 10.1038/nature02040. [PubMed: 14574413]
4. Shiozawa Y, Pedersen EA, Havens AM, Jung Y, Mishra A, Joseph J, et al. Human prostate cancer metastases target the hematopoietic stem cell niche to establish footholds in mouse bone marrow. J Clin Invest 2011;121(4):1298–312 doi 10.1172/JCI43414. [PubMed: 21436587]
5. Tucker RP, Drabikowski K, Hess JF, Ferralli J, Chiquet-Ehrismann R, Adams JC. Phylogenetic analysis of the tenascin gene family: evidence of origin early in the chordate lineage. BMC Evol Biol 2006;6:60 doi 10.1186/1471-2148-6-60 [pii] 10.1186/1471-2148-6-60. [PubMed: 16893461]
6. Mackie EJ, Murphy LI. The role of tenascin-C and related glycoproteins in early chondrogenesis. Microsc Res Tech 1998;43(2):102–10 doi 10.1002/(SICI)1097-0029(19981015)43:2<102::AID-JEMT3>3.0.CO;2-T. [PubMed: 9822997]
7. Chiquet-Ehrismann R, Mackie EJ, Pearson CA, Sakakura T. Tenascin: an extracellular matrix protein involved in tissue interactions during fetal development and oncogenesis. Cell 1986;47(1):131–9. [PubMed: 2428505]
8. Hakkinen L, Hildebrand HC, Berndt A, Kosmehl H, Larjava H. Immunolocalization of tenascin-C, alpha9 integrin subunit, and alphavbeta6 integrin during wound healing in human oral mucosa. J Histochem Cytochem 2000;48(7):985–98. [PubMed: 10858276]
9. Okamura N, Hasegawa M, Nakoshi Y, Iino T, Sudo A, Imanaka-Yoshida K, et al. Deficiency of tenascin-C delays articular cartilage repair in mice. Osteoarthritis Cartilage 2010;18(6):839–48 doi 10.1016/j.joca.2009.08.013. [PubMed: 19747998]
10. Mackie EJ, Halfter W, Liverani D. Induction of tenascin in healing wounds. J Cell Biol 1988;107(6 Pt 2):2757–67. [PubMed: 2462568]
11. Mackie EJ, Abraham LA, Taylor SL, Tucker RP, Murphy LI. Regulation of tenascin-C expression in bone cells by transforming growth factor-beta. Bone 1998;22(4):301–7. [PubMed: 9556128]
12. Mackie EJ, Thesleff I, Chiquet-Ehrismann R. Tenascin is associated with chondrogenic and osteogenic differentiation in vivo and promotes chondrogenesis in vitro. J Cell Biol 1987;105(6 Pt 1):2569–79. [PubMed: 2447094]
13. Kilian O, Dahse R, Alt V, Zardi L, Hentschel J, Schnettler R, et al. mRNA expression and protein distribution of fibronectin splice variants and high-molecular weight tenascin-C in different phases of human fracture healing. Calcified tissue international 2008;83(2):101–11 doi 10.1007/s00223-008-9156-z. [PubMed: 18663401]
14. Tuxhorn JA, Ayala GE, Smith MJ, Smith VC, Dang TD, Rowley DR. Reactive stroma in human prostate cancer: induction of myofibroblast phenotype and extracellular matrix remodeling. Clin Cancer Res 2002;8(9):2912–23. [PubMed: 12231536]

15. Desmouliere A, Chaponnier C, Gabbiani G. Tissue repair, contraction, and the myofibroblast. Wound Repair Regen 2005;13(1):7–12 doi WRR130102 [pii] 10.1111/j.1067-1927.2005.130102.x. [PubMed: 15659031]
16. Kim W, Barron DA, San Martin R, Chan KS, Tran LL, Yang F, et al. RUNX1 is essential for mesenchymal stem cell proliferation and myofibroblast differentiation. Proc Natl Acad Sci U S A 2014;111(46):16389–94 doi 10.1073/pnas.1407097111. [PubMed: 25313057]
17. Midwood KS, Orend G. The role of tenascin-C in tissue injury and tumorigenesis. J Cell Commun Signal 2009;3(3–4):287–310 doi 10.1007/s12079-009-0075-1. [PubMed: 19838819]
18. Jachetti E, Caputo S, Mazzoleni S, Brambillasca CS, Parigi SM, Grioni M, et al. Tenascin-C Protects Cancer Stem-like Cells from Immune Surveillance by Arresting T-cell Activation. Cancer Res 2015;75(10):2095–108 doi 10.1158/0008-5472.CAN-14-2346. [PubMed: 25808872]
19. Tuxhorn JA, Ayala GE, Rowley DR. Reactive stroma in prostate cancer progression. J Urol 2001;166(6):2472–83. [PubMed: 11696814]
20. Ayala GE, Tuxhorn JA, Wheeler TM, Frolov A, Scardino PT, Ohori M, et al. Reactive stroma as a predictor of biochemical free recurrence in prostate cancer. Clin Cancer Res 2003;9:4792–801. [PubMed: 14581350]
21. Schauer IG, Ressler SJ, Tuxhorn JA, Dang TD, Rowley DR. Elevated epithelial expression of interleukin-8 correlates with myofibroblast reactive stroma in benign prostatic hyperplasia. Urology 2008;72(1):205–13. [PubMed: 18314176]
22. Huang W, Chiquet-Ehrismann R, Moyano JV, Garcia-Pardo A, Orend G. Interference of tenascin-C with syndecan-4 binding to fibronectin blocks cell adhesion and stimulates tumor cell proliferation. Cancer Res 2001;61(23):8586–94. [PubMed: 11731446]
23. Bubendorf L, Schopfer A, Wagner U, Sauter G, Moch H, Willi N, et al. Metastatic patterns of prostate cancer: an autopsy study of 1,589 patients. Hum Pathol 2000;31(5):578–83. [PubMed: 10836297]
24. Paget S. The distribution of secondary growths in cancer of the breast. 1889. Cancer metastasis reviews 1989;8(2):98–101.
25. Bonfil RD, Chinni S, Fridman R, Kim HR, Cher ML. Proteases, growth factors, chemokines, and the microenvironment in prostate cancer bone metastasis. Urologic oncology 2007;25(5):407–11 doi 10.1016/j.urolonc.2007.05.008. [PubMed: 17826661]
26. Probstmeier R, Pesheva P. Tenascin-C inhibits beta1 integrin-dependent cell adhesion and neurite outgrowth on fibronectin by a disialoganglioside-mediated signaling mechanism. Glycobiology 1999;9(2):101–14. [PubMed: 9949188]
27. Schneider CA, Rasband WS, Eliceiri KW. NIH Image to ImageJ: 25 years of image analysis. Nature methods 2012;9(7):671–5. [PubMed: 22930834]
28. Taooka Y, Chen J, Yednock T, Sheppard D. The integrin alpha9beta1 mediates adhesion to activated endothelial cells and transendothelial neutrophil migration through interaction with vascular cell adhesion molecule-1. J Cell Biol 1999;145(2):413–20. [PubMed: 10209034]
29. Li M, Pathak RR, Lopez-Rivera E, Friedman SL, Aguirre-Ghiso JA, Sikora AG. The In Ovo Chick Chorioallantoic Membrane (CAM) Assay as an Efficient Xenograft Model of Hepatocellular Carcinoma. J Vis Exp 2015(104) doi 10.3791/52411.
30. Morgan JM, Wong A, Yellowley CE, Genetos DC. Regulation of tenascin expression in bone. J Cell Biochem 2011;112(11):3354–63 doi 10.1002/jcb.23265. [PubMed: 21751239]
31. Webb CM, Zaman G, Mosley JR, Tucker RP, Lanyon LE, Mackie EJ. Expression of tenascin-C in bones responding to mechanical load. J Bone Miner Res 1997;12(1):52–8 doi 10.1359/jbmr.1997.12.1.52. [PubMed: 9240725]
32. Sung SY, Hsieh CL, Law A, Zhau HE, Pathak S, Multani AS, et al. Coevolution of prostate cancer and bone stroma in three-dimensional coculture: implications for cancer growth and metastasis. Cancer Res 2008;68(23):9996–10003 doi 68/23/9996 [pii] 10.1158/0008-5472.CAN-08-2492. [PubMed: 19047182]
33. Yu C, Shiozawa Y, Taichman RS, McCauley LK, Pienta K, Keller E. Prostate cancer and parasitism of the bone hematopoietic stem cell niche. Crit Rev Eukaryot Gene Expr 2012;22(2):131–48. [PubMed: 22856431]

34. Nakamura-Ishizu A, Okuno Y, Omatsu Y, Okabe K, Morimoto J, Uede T, et al. Extracellular matrix protein tenascin-C is required in the bone marrow microenvironment primed for hematopoietic regeneration. Blood 2012;119(23):5429–37 doi 10.1182/blood-2011-11-393645. [PubMed: 22553313]
35. Adams JC, Chiquet-Ehrismann R, Tucker RP. The evolution of tenascins and fibronectin. Cell Adh Migr 2015;9(1–2):22–33 doi 10.4161/19336918.2014.970030. [PubMed: 25482621]
36. Nemeth JA, Harb JF, Barroso U Jr., He Z, Grignon DJ, Cher ML. Severe combined immunodeficient-hu model of human prostate cancer metastasis to human bone. Cancer Res 1999;59(8):1987–93. [PubMed: 10213511]
37. Schaffler MB, Choi K, Milgrom C. Aging and matrix microdamage accumulation in human compact bone. Bone 1995;17(6):521–25. [PubMed: 8835305]
38. Siegel RL, Miller KD, Jemal A. Cancer statistics, 2015. CA Cancer J Clin 2015;65(1):5–29 doi 10.3322/caac.21254.
39. Boorjian SA, Thompson RH, Tollefson MK, Rangel LJ, Bergstralh EJ, Blute ML, et al. Long-term risk of clinical progression after biochemical recurrence following radical prostatectomy: the impact of time from surgery to recurrence. Eur Urol 2011;59(6):893–9 doi 10.1016/j.eururo.2011.02.026. [PubMed: 21388736]
40. Danila DC, Heller G, Gignac GA, Gonzalez-Espinoza R, Anand A, Tanaka E, et al. Circulating tumor cell number and prognosis in progressive castration-resistant prostate cancer. Clin Cancer Res 2007;13(23):7053–8 doi 10.1158/1078-0432.CCR-07-1506. [PubMed: 18056182]
41. van der Toom EE, Verdone JE, Pienta KJ. Disseminated tumor cells and dormancy in prostate cancer metastasis. Curr Opin Biotechnol 2016;40:9–15 doi 10.1016/j.copbio.2016.02.002. [PubMed: 26900985]
42. Shiozawa Y, Berry JE, Eber MR, Jung Y, Yumoto K, Cackowski FC, et al. The marrow niche controls the cancer stem cell phenotype of disseminated prostate cancer. Oncotarget 2016;7(27):41217–32 doi 10.18632/oncotarget.9251. [PubMed: 27172799]
43. Mittan D, Lee S, Miller E, Perez RC, Basler JW, Bruder JM. Bone loss following hypogonadism in men with prostate cancer treated with GnRH analogs. J Clin Endocrinol Metab 2002;87(8):3656–61 doi 10.1210/jcem.87.8.8782. [PubMed: 12161491]
44. Greenspan SL, Coates P, Sereika SM, Nelson JB, Trump DL, Resnick NM. Bone loss after initiation of androgen deprivation therapy in patients with prostate cancer. J Clin Endocrinol Metab 2005;90(12):6410–7 doi 10.1210/jc.2005-0183. [PubMed: 16189261]
45. Ruppender N, Larson S, Lakely B, Kollath L, Brown L, Coleman I, et al. Cellular Adhesion Promotes Prostate Cancer Cells Escape from Dormancy. PLoS One 2015;10(6):e0130565 doi 10.1371/journal.pone.0130565.
46. Ota D, Kanayama M, Matsui Y, Ito K, Maeda N, Kutomi G, et al. Tumor-alpha9beta1 integrin-mediated signaling induces breast cancer growth and lymphatic metastasis via the recruitment of cancer-associated fibroblasts. J Mol Med (Berl) 2014;92(12):1271–81 doi 10.1007/s00109-014-1183-9. [PubMed: 25099519]
47. Ioachim E, Charchanti A, Briasoulis E, Karavasilis V, Tsanou H, Arvanitis DL, et al. Immunohistochemical expression of extracellular matrix components tenascin, fibronectin, collagen type IV and laminin in breast cancer: their prognostic value and role in tumour invasion and progression. Eur J Cancer 2002;38(18):2362–70. [PubMed: 12460779]
48. Oskarsson T, Acharyya S, Zhang XH, Vanharanta S, Tavazoie SF, Morris PG, et al. Breast cancer cells produce tenascin C as a metastatic niche component to colonize the lungs. Nat Med 2011;17(7):867–74 doi 10.1038/nm.2379. [PubMed: 21706029]
49. Sun X, Fa P, Cui Z, Xia Y, Sun L, Li Z, et al. The EDA-containing cellular fibronectin induces epithelial-mesenchymal transition in lung cancer cells through integrin alpha9beta1-mediated activation of PI3-K/AKT and Erk1/2. Carcinogenesis 2014;35(1):184–91 doi 10.1093/carcin/bgt276. [PubMed: 23929437]
50. Gulubova M, Vlaykova T. Immunohistochemical assessment of fibronectin and tenascin and their integrin receptors alpha5beta1 and alpha9beta1 in gastric and colorectal cancers with lymph node and liver metastases. Acta Histochem 2006;108(1):25–35 doi 10.1016/j.acthis.2005.12.001. [PubMed: 16430945]

51. Mambole A, Bigot S, Baruch D, Lesavre P, Halbwachs-Mecarelli L. Human neutrophil integrin alpha9beta1: up-regulation by cell activation and synergy with beta2 integrins during adhesion to endothelium under flow. J Leukoc Biol 2010;88(2):321–7 doi 10.1189/jlb.1009704. [PubMed: 20435742]

52. Chiquet M, Birk DE, Bonnemann CG, Koch M. Collagen XII: Protecting bone and muscle integrity by organizing collagen fibrils. Int J Biochem Cell Biol 2014;53:51–4 doi 10.1016/j.biocel.2014.04.020. [PubMed: 24801612]

53. Bader HL, Keene DR, Charvet B, Veit G, Driever W, Koch M, et al. Zebrafish collagen XII is present in embryonic connective tissue sheaths (fascia) and basement membranes. Matrix Biol 2009;28(1):32–43 doi 10.1016/j.matbio.2008.09.580. [PubMed: 18983916]

54. Izu Y, Ezura Y, Koch M, Birk DE, Noda M. Collagens VI and XII form complexes mediating osteoblast interactions during osteogenesis. Cell Tissue Res 2016;364(3):623–35 doi 10.1007/s00441-015-2345-y. [PubMed: 26753503]

55. Izu Y, Sun M, Zwolanek D, Veit G, Williams V, Cha B, et al. Type XII collagen regulates osteoblast polarity and communication during bone formation. J Cell Biol 2011;193(6):1115–30 doi 10.1083/jcb.201010010. [PubMed: 21670218]

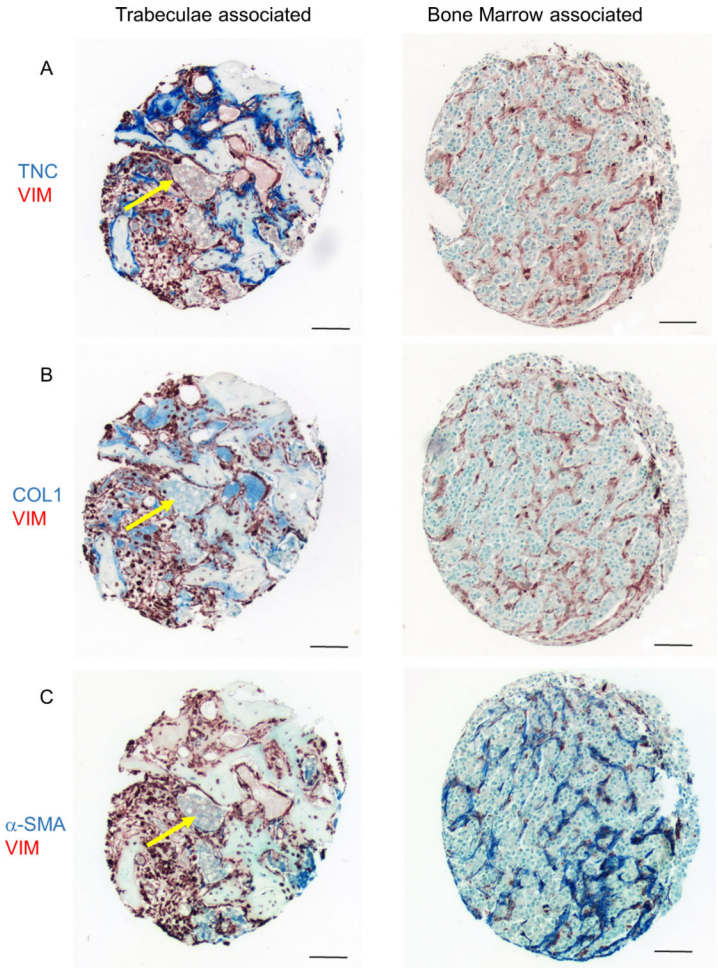

Figure 1. Characterization of the reactive endosteum phenotype in prostate derived bone metastasis

Bone metastasis tissue arrays were stained for reactive stroma markers. Characteristic trabeculae – associated and bone marrow metastasis samples shown. Metastatic foci denoted with arrows. Scale bar 100 μm.

A) Tenascin-C (AP-Vector Blue)-Vimentin (HRP-Nova Red)

B) Pro Collagen I (AP-Vector Blue)-Vimentin (HRP-Nova Red)

C) Smooth Muscle Alpha Actin (AP-Vector Blue)-Vimentin (HRP-Nova Red)

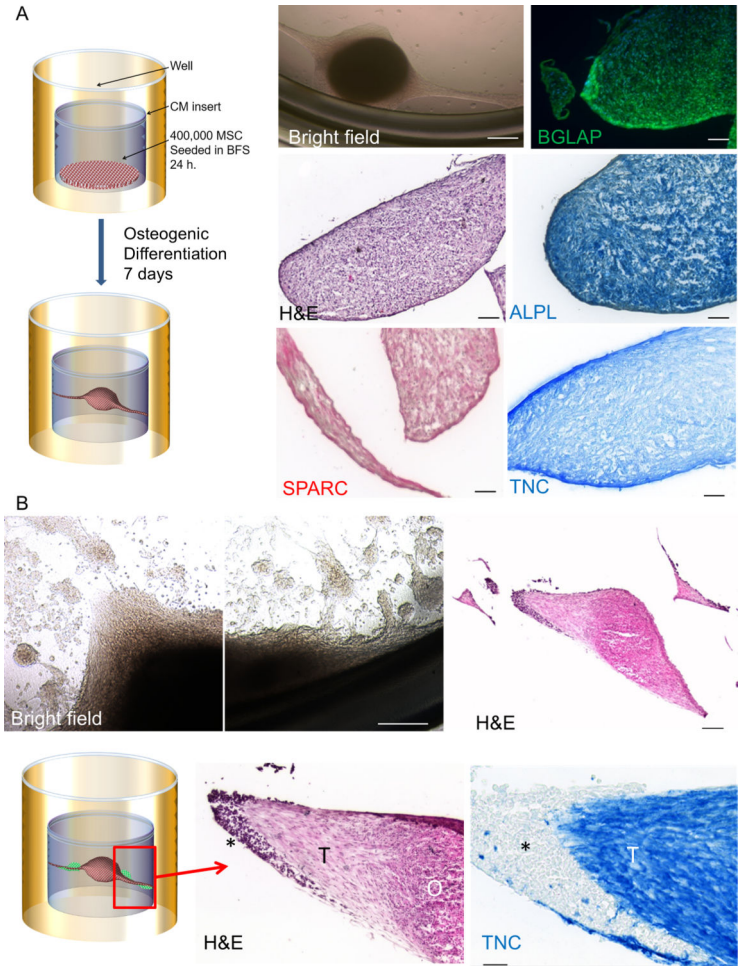

Figure 2. MSC-derived osteogenic organoid and its interactions with the prostate cancer - derived metastatic cell line VCaP.

A mesenchymal stem cell-derived osteogenic three-dimensional spheroid model was developed to generate a fully defined, human model system where cancer and endosteum compartments are easily manipulated.

A) Experimental protocol for organoid development. After seven days of induction, organoids turn hard and opalescent, and develop endosteal tendrils. Bright field image, scale bar 200 μm. The osteogenic organoid expresses osteoblast-specific markers: IF. Osteocalcin (BGLAP) FITC. DAPI nuclear counterstain. H&E. IHC alkaline phosphatase (ALPL), osteonectin (SPARC) and tenascin-C (TNC) Scale bar 100 μm.

B) Co-culture of the osteogenic organoid with the metastatic cell line VCaP. Cancer cells (*) associate at the sites of highest tenascin-C deposition, closer to the endosteal tendrils (T). Bright field. Scale bar 500 μm. H&E scale bar 250 μm and 50 μm. IHC Tenascin-C, Scale bar 50 μm.

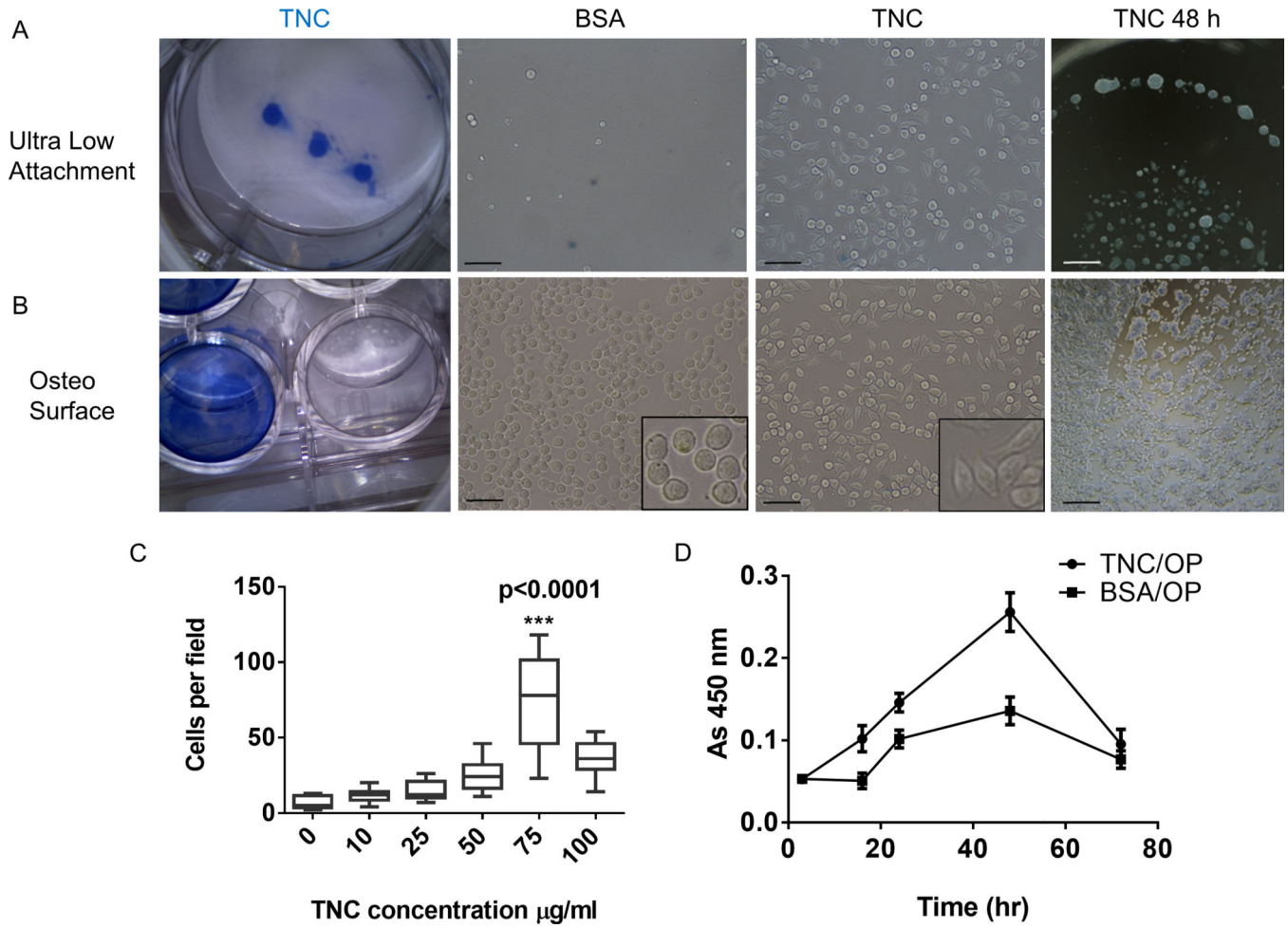

Figure 3. VCaP adhesion and spreading in ultra-low attachment and osteo mimetic plates is enhanced by tenascin-C coating.

A) VCaP adhesion in ultra-low attachment plates. Confirmation of tenascin-C coating by immunocytochemistry (AP-Blue). VCaP attachment (3 hours) in tenascin-C or BSA control. Note that cells flatten out and spread on tenascin-C and they do not lift from ULA plates after washing. Scale bar 25 µm

B) VCaP adhesion in osteo mimetic plates. Confirmation of tenascin-C coating by immunocytochemistry. VCaP attachment (3 hours) to tenascin-C Scale bar 25 µm. VCaP culture on tenascin-C coated surfaces form three dimensional foci in non-serum containing media at 48 hr. regardless of culture surface type. Scale bar 50 µm

C) VCaP attachment to tenascin-C is concentration dependent. Summary of three independent experiments analyzing cell number after 24-hour culture in osteo surfaces, data represents mean values ±SEM. ***$p<0.001$

D) VCaP cells attach and initiate proliferation sooner on tenascin-C coated osteo mimetic plates and reach higher density relative to control (BSA-coated) conditions in serum-free media. Summary of four independent experiments analyzing cell proliferation on osteo surfaces via MTT assay, data represents mean values ±SEM, $p<0.0001$.

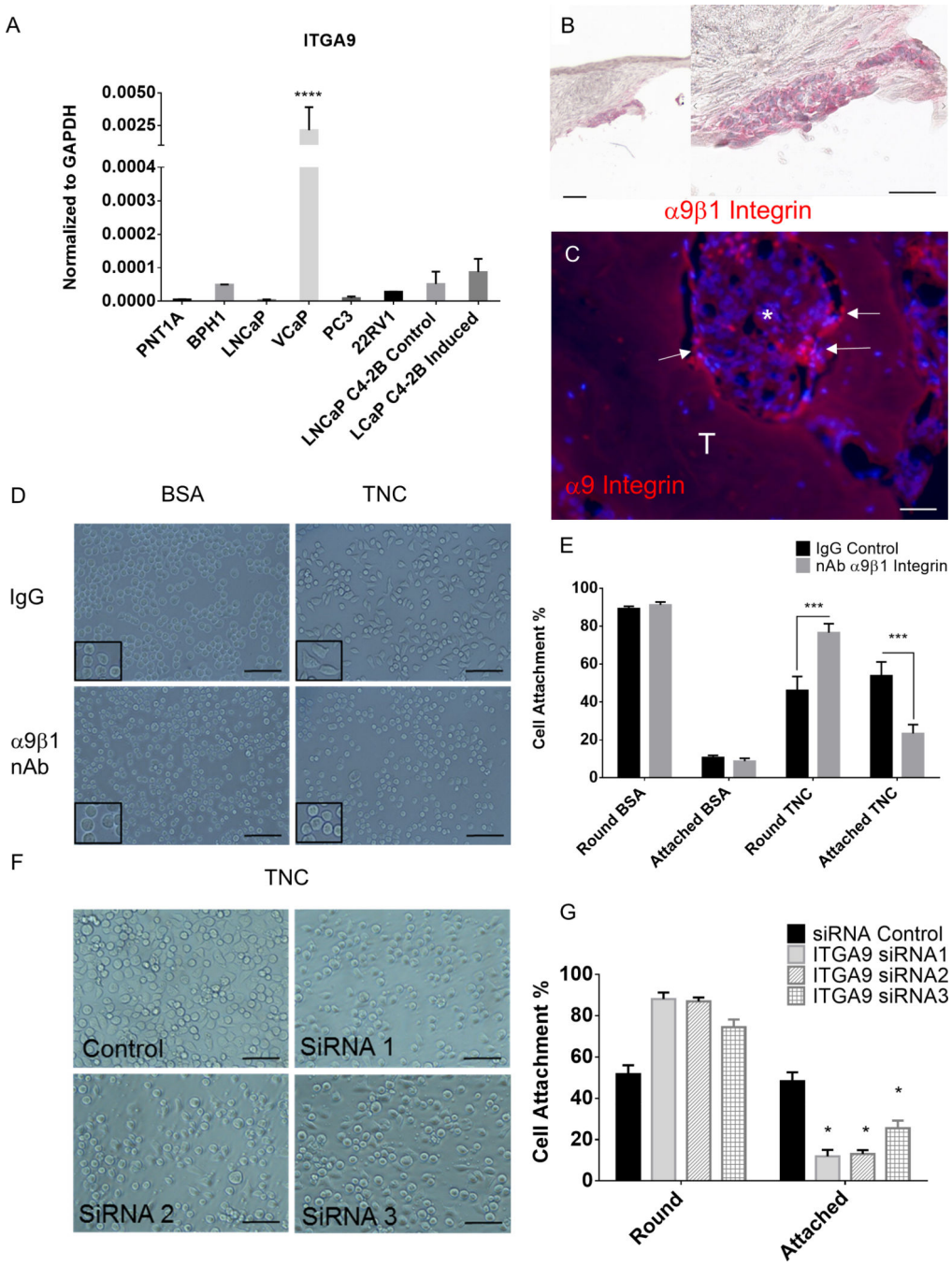

Figure 4. VCaP adhesion to tenascin-C is mediated by α9β1 integrin.

A) The metastatic prostate cell line VCaP expresses a significantly higher amount of integrin alpha nine when compared to other prostate cell lines. RT-QPCR Data represents mean values ±SEM, **** $p<0.0001$

B) Staining for the α9β1 dimer in the osteogenic organoid co culture. Scale bar 100 μm

C) Staining for α9 Integrin (Texas Red) in the human metastasis prostate array. Image shows an adjacent section to the sample shown in Figure 1. Metastatic foci (*) shown associated to trabecular bone (T). ITGA9 cells denoted by arrows. Scale bar 100 μm.

D) Neutralization of α9β1 via a neutralizing antibody ablates attachment to tenascin-C in VCaP.

E) Summary of three independent α9β1 neutralization experiments on tenascin-C coated osteo surfaces data represents mean values ±SEM. ***p<0.001

F) Neutralization of alpha 9 integrin via SiRNA ablates VCaP attachment to tenascin-C

G) Summary of three independent α9β1 knockdown-adhesion experiments on tenascin-C-coated osteo surfaces, data represents mean values ±SEM.*p<0.05.

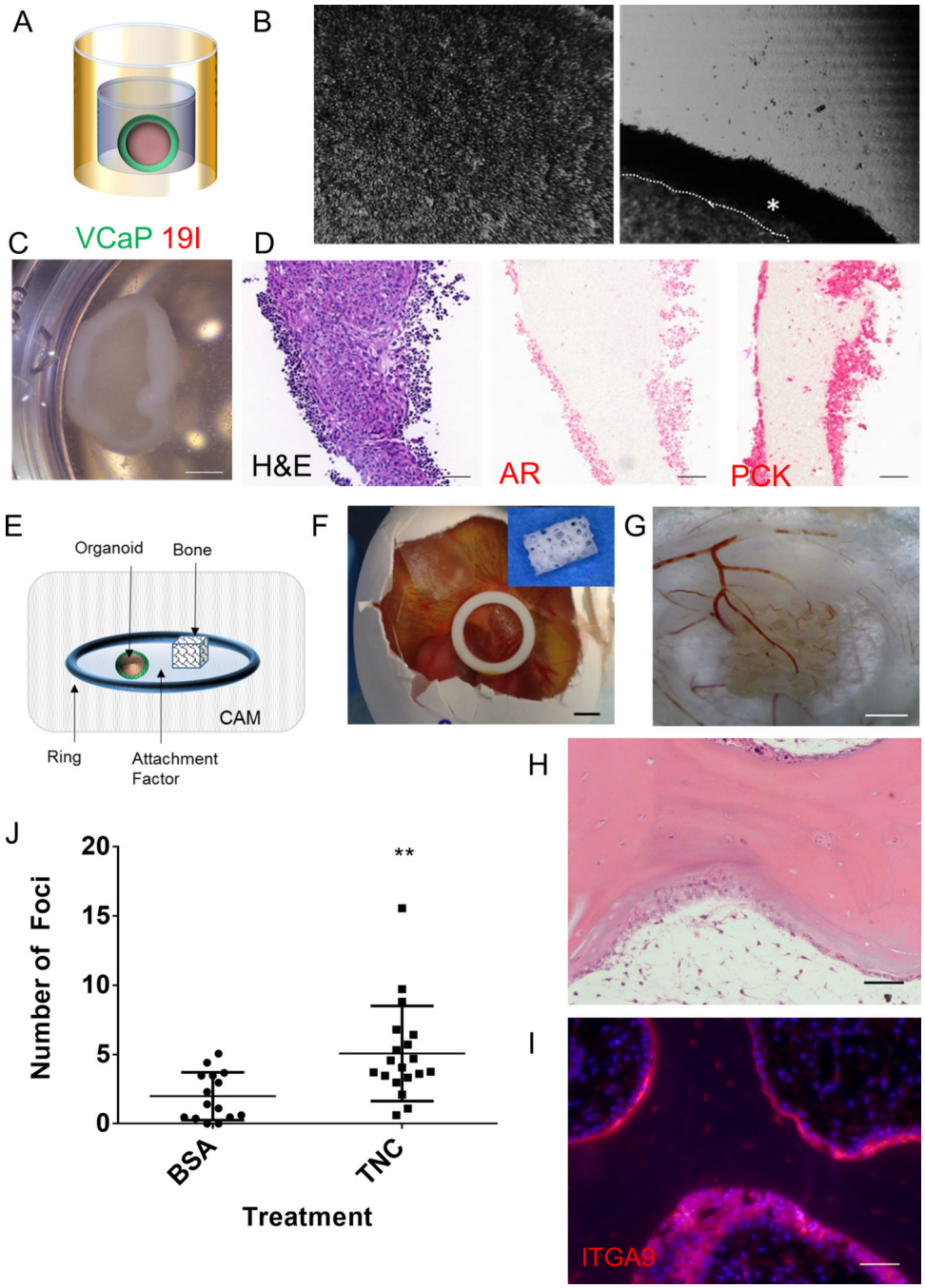

Figure 5. The CAM- Humanized Bovine Bone integrated experimental system shows preferential cancer cell chemotaxis and colonization bone scaffolds enriched in tenascin-C

A) Graphic representation of the prostate epithelial-stroma organoid structure. Distinct hpMSC 19-I (stroma) internal compartment self-segregates from an epithelial mantle.

B) Formation of the prostate epithelial-stroma organoid. A mixture of hpMSC 19-I and VCaP is seeded in suspension in non-adhesive conditions. Two hours after seeding, the organoid contracts and segregation of the epithelial (*) and the stromal compartments occurs (Stromal-epithelial border highlighted by dotted line). Images captured with the CytoSmart live cell imaging system (Lonza).

C) Bright field image of the organoid at 24-hour incubation. Scale bar 500 μm
D) Serial sections of the prostate organoid: H&E. IHC for androgen receptor (AR) and pan-cytokeratin (PCK) denote the epithelial compartment of the organoid. Scale bar 100 μm
E) Experimental setup of the *in ovo* xenograft system
F) Trabecular bone scaffold *in ovo*. Inset: Trabecular bone scaffold. Scale bar 5 mm
G) Bulk dissection of the xenograft. Tenascin-C coated bone xenograft after 6 days of incubation *in ovo.* The bone fragment associates with the CAM. Blood vessels infiltrate the trabecular bone xenograft. Scale bar 2.5 mm
H, I) Serial sections of CAM associated-bone xenograft is colonized by VCaP. H&E, IF α9 integrin (Texas Red), tissue counterstained with DAPI scale bar 100 μm
J) Summary of eight independent experiments (19 tenascin-C samples, 15 control), analyzing the number of VCaP foci associated to bone xenografts shows preferential recruitment to tenascin-C coated scaffolds. ***$p<0.001$

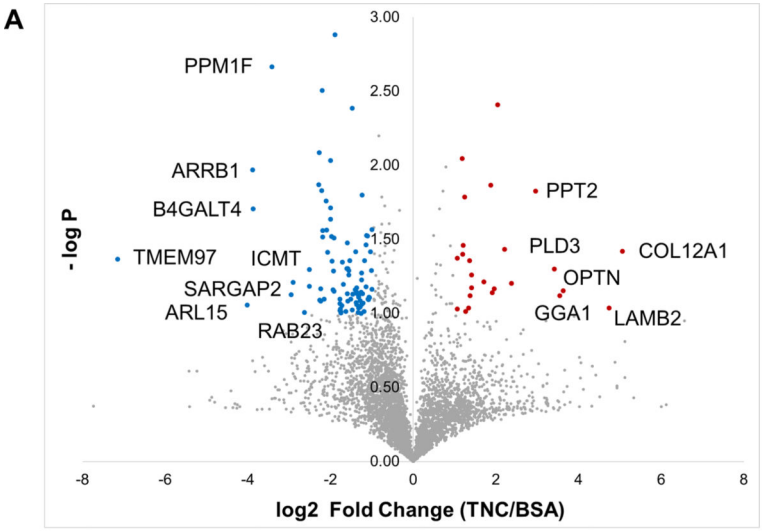

Gene ID	Gene Symbol	log2 fold
1303	COL12A1	5.06
3913	LAMB2	4.73
10133	OPTN	3.63
26088	GGA1	3.55
23646	PLD3	3.42
9374	PPT2	2.96
51715	RAB23	-2.64
23463	ICMT	-2.90
23380	SRGAP2	-2.95
9647	PPM1F	-3.42
8702	B4GALT4	-3.87
408	ARRB1	-3.89
54622	ARL15	-4.02
27346	TMEM97	-7.15

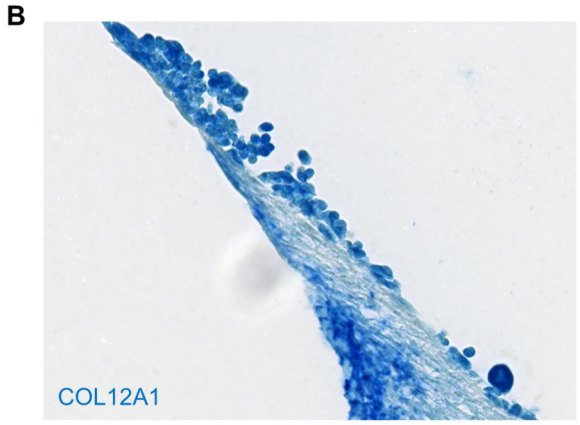

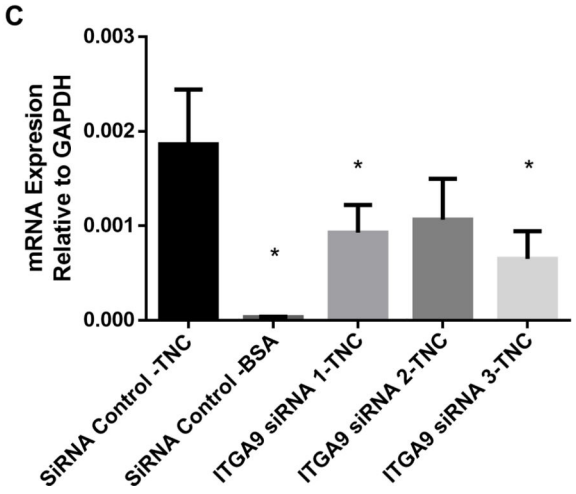

Figure 6. Differential protein expression in VCaP cultured in tenascin-C-Osteo plate.

A) Mass spectrometry reveals enhanced expression of Collagen 12A and Laminin beta 2 subunit in VCaP because of culture on tenascin-C coated osteo surfaces

B) VCaP that associate with the osteogenic organoid express COL12A1. IHC COL12A1

C) Ablation of adhesion via Integrin α9 knock out decreases expression of COL12A1 in VCaP when cells are cultured on tenascin-C coated osteo mimetic surfaces. Summary of three independent RT PCR studies on the expression of COL12A1 upon ITGA9 knock out *p<0.05